ENGINE EXHAUST NOZZLE PLUME EFFECTS ON THE SONIC BOOM FOR A TYPE OF HYPERSONIC LONG-RANGE CIVIL VEHICLE

Qian Zhansen[a,b], Leng Yan[a,b], Liu Zhongchen[a,b]
[a]**AVIC Aerodynamics Research Institute, Shenyang, 110034, China**
[b]**Aviation Key Laboratory of Science and Technology on High Speed and High Reynolds Number Aerodynamic Force Research, Shenyang, 110034, China**

Keywords: *hypersonic, sonic boom, nozzle plume, long-range civil vehicle*

Abstract

Based on a type of hypersonic civil vehicle, engine exhaust nozzle plume are considered for investigating their effects on the sonic boom overpressure and duration on the ground. Here, the parameters include nozzle pressure ratio (NPR) and Mach number. This work is accomplished through computational fluid dynamics (CFD) analysis. The near-field flows are calculated by the ARI_Overset CFD solver of AVIC ARI which is based on the Navier-Stokes equations. The characteristics of the ground sonic boom are calculated by the waveform parameter method (WPM) developed by Thomas. Both Mach number and NPR are varied in this work, and the amplitude of overpressure and duration on the ground is obtained to evaluate the plume effects on the sonic boom.

1 Introduction

For a supersonic aircraft, in the near-field flow there exist a series of complicated pressure waves, such as shock waves, contact discontinuities or expansion fans, which originate from various parts of the airframe and engine. At the vehicle nose, there is a rise in pressure followed by a steady decrease to negative pressure, and then rising to atmospheric pressure. When propagated to the ground, these waves coalesce into the characteristic N-shaped wave. The two large pressure changes create a “double boom” effect [1]. Figure 1 shows a schematic of the generation and propagation of sonic boom from the aircraft.

The impact of the sonic boom is so large that the Federal Aviation Administration (FAA) has issued a noise policy in Federal Aviation Regulation (FAR) Part 91 item 817 for supersonic aircraft stating: "Since March 1973, supersonic flight over land by civil or private aircraft has been prohibited by regulation in the United States." In order to avoid negative impact of sonic boom on people, the same policy also states in other nations and regions. The sonic boom is one of the most important challenges for hypersonic vehicle.

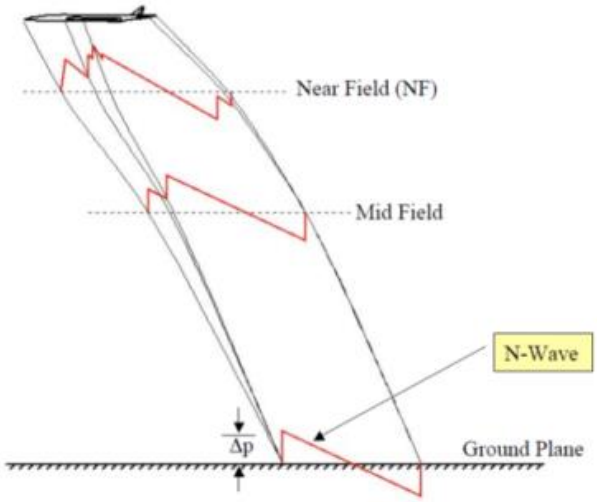

Fig. 1 Sonic boom generation and propagation

In recent years, the sonic boom signature generated by the forward shocks has been investigated widely, such as the Shaped Sonic Boom Demonstration (SSBD) project [2] sponsored by DARPA. So, some works need to be done for the trailing shocks. The trailing shock will directly affect the right-hand portion of the sonic boom N wave. Many factors are included in the aft body, such as tail, nacelles

and nozzle, in which the nozzle plume is one of the most important factors.

In this paper, computational fluid dynamics (CFD) is utilized to analyze the nozzle plume effects on the sonic boom. Both Mach number and nozzle pressure ratio (NPR) are varied in this work, and the characteristics of the ground sonic boom are shown.

2 Numerical approaches

2.1 Near-field calculation

Near-field solution at the flying altitude is obtained by solving the conservative Navier-Stokes equations using ARI_Overset in-house CFD solver developed by AVIC ARI [3,4]. In order to guarantee the accuracy of computations and save the computation cost, grid adaptation is used to cluster grid lines towards the regions around the shocks. The spatial discretization involves a semi-discrete cell-centered finite volume method. The AUSMDV flux-difference splitting scheme evaluate the convective fluxes and 2nd order scheme is used to interpolate flow variables to the interface of the control volume. Temporal advancement is implicit. The computational mesh is hybrid grids which are generated by commercial software POINTWISE [5].

2.2 Far-field computation

Acoustic rays are emitted from the aircraft and propagate orthogonally to the wavefront. They represent the paths along which the acoustic disturbance propagates in atmosphere. The initial direction of a ray is given by the ray cone near the aircraft which is orthogonal to the Mach cone. Based on ray tracing algorithm, near-field pressure signatures are extrapolated to the ground level through the waveform parameter method developed by Thomas [6]. In this method, the pressure wave is approximated by an arbitrary number of linear segments and each segment is characterized by three parameters (see Fig. 2):

• m_i the slope of pressure waveform of segment i

• Δp_i the pressure rise across shock at the juncture of segment i and $i-1$

• λ_i the time duration of segment i

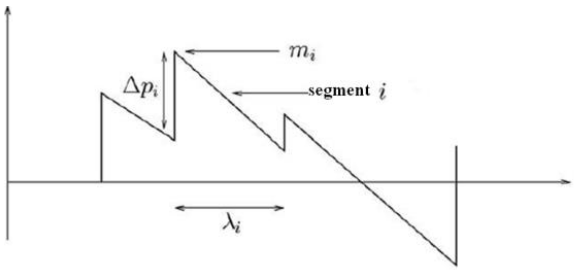

Fig. 2 Illustration of the waveform parameters

Three ordinary, first-order, coupled differential equations which completely describe the deformation of the waveform for the waveform parameters are as follows:

$$\frac{dm_i}{dt} = C_1 m_i^2 + C_2 m_i$$

$$\frac{d\Delta p_i}{dt} = \frac{1}{2} C_1 \Delta p_i (m_i + m_{i-1}) + C_2 \Delta p_i$$

$$\frac{d\lambda_i}{dt} = -\frac{1}{2} C_1 (\Delta p_i + \Delta p_{i+1}) - C_1 m_i \lambda_i$$

where

$$C_1 = \frac{\gamma+1}{2\gamma}\frac{a_0}{p_0 c_n};\quad C_2 = \frac{1}{2}\left(\frac{3}{a_0}\frac{da_0}{dt} + \frac{1}{\rho_0}\frac{d\rho_0}{dt} - \frac{2}{c_n}\frac{dc_n}{dt} - \frac{1}{A}\frac{dA}{dt}\right)$$

For the above equations, a_0, p_0, ρ_0 are the sound speed, pressure and density for the flight altitude respectively; $c_n = a_0 + \vec{V}_0 \cdot \vec{N}$ is the wave propagation speed along the acoustic ray cone; A is the acoustic ray tube area. All these quantities are functions only of the altitude and therefore vary along the ray tube.

In a non-uniform atmosphere with winds, the quantities C_1 and C_2 vary along the ray path in the case of a wave with arbitrary wavefront shape. However, if assumed to be constant over small time increments, the above equations can be integrated to obtain the following solution:

$$\lambda_i = (1 - C_1 m_i^0 T)\left[\lambda_i^0 - \frac{\Delta p_i^0}{m_i^0 - m_{i-1}^0}\left(\sqrt{\frac{1 - C_1 m_{i-1}^0 T}{1 - C_1 m_i^0 T}} - 1\right) - \frac{\Delta p_{i+1}^0}{m_i^0 - m_{i+1}^0}\left(\sqrt{\frac{1 - C_1 m_{i+1}^0 T}{1 - C_1 m_i^0 T}} - 1\right)\right]$$

$$\Delta p_i = \frac{\Delta p_i^0 e^{C_2 \Delta t}}{[(1 - C_1 m_i^0 T)(1 - C_1 m_{i-1}^0 T)]^{1/2}}$$

$$m_i = \frac{m_i^0 e^{C_2 \Delta t}}{1 - C_1 m_i^0 T}$$

where $T = \dfrac{e^{C_2 \Delta t} - 1}{C_2}$.

From above solutions, it is clear that one must first calculate the values of C_1, C_2 at many interested points by given $m_i^0, \Delta p_i^0, \lambda_i^0$, and the key is the fractional rate of change of the properties a_0, p_0, ρ_0, c_n at the fighting altitude. Ray tube area can be determined directly by independently calculating each of the four rays that bound the ray tube. Detailed formulae to compute ray path is given in [7].

3 Sonic boom prediction and analysis

3.1 Model and grid

The three views of computational model are seen in figure 3. The hypersonic long-range transport vehicle [8,9] which is assumed to have a reference length $L = 17.405m$ has the top mounted inlet aerodynamic configuration. The designed flight condition of this vehicle is Ma=6.0 with flight altitude of H=27*km*, and the designed nozzle pressure ratio (NPR) is 1000. The total mesh element number used in this work is about 55 million. Figure 4 shows the grids in symmetry plane.

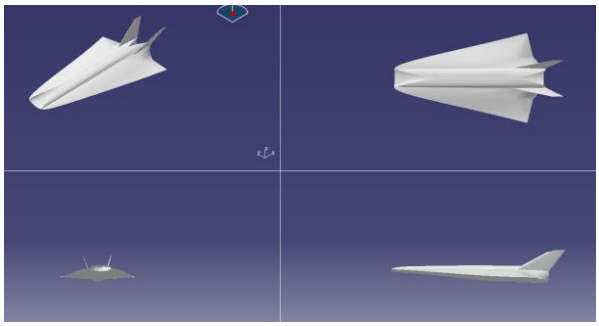

Fig. 3 Three views of hypersonic transport vehicle

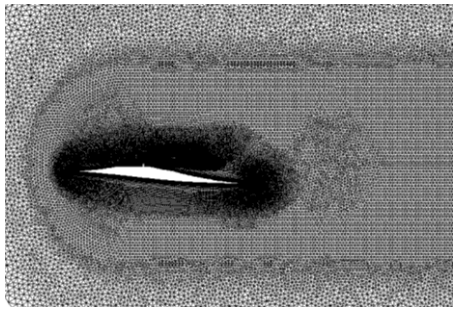

Fig. 4 The grids in symmetry plane

3.2 Numerical method validation

In order to validate the accuracy of above numerical approach, double-cone [10,11] is used as a verification case. The geometry of the double-cone is shown in figure 5. Signature got in $h/L = 5$ with Mach number of 1.41 is compared with experimental data [10] as shown in figure 6. The computational solutions and the measured results are in good agreement generally. This illuminates that the ARI_Overset software and its approach is credible.

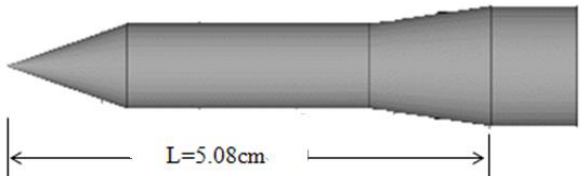

Fig. 5 Side-View of the double-cone configuration

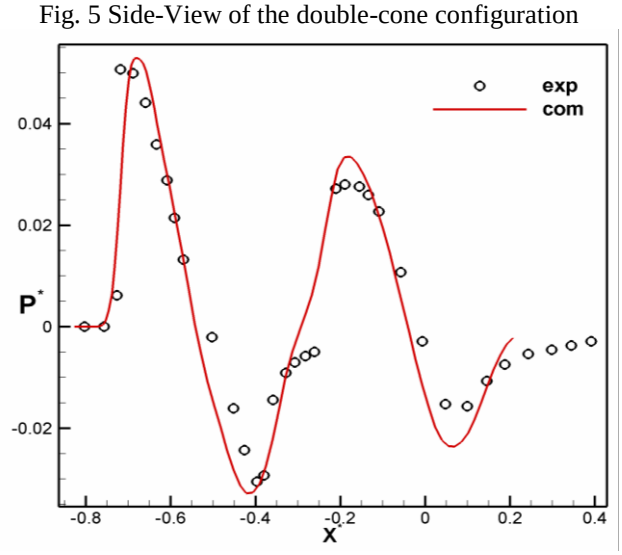

Fig. 6 Compared of experimental data to the present numerical solutions at $h/L = 5$

3.3 Numerical results analysis

In the present investigation, the characteristic parameters of sonic boom considered are overpressure (dp (+) and dp (-)), peak-to-peak magnitude [12,13] and time duration on the ground, depicted in figure 7. All the calculated cases are summarized in table 1 in the process of near-field simulation, and the pressure distributions at zero angle of attack taken at $h/L = 1.15$ from the model, where h is the distance to the model center line. For all the cases, the data at $h/L = 1.15$ are used as initial value for propagating to far-field.

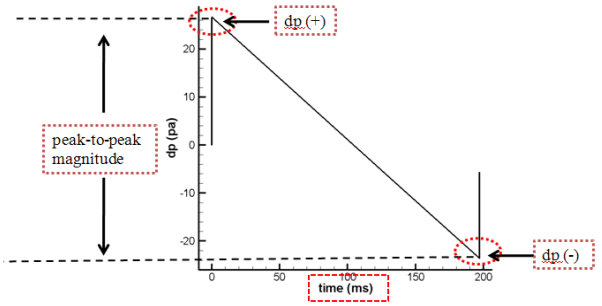

Fig. 7 The characteristics of sonic boom considered

Table 1 All ran cases for near-field simulation

Case	Ma	Altitude/km	NPR
1	5	21	50, 200, 600, 1000, 1500, 2000
2	6	27	50, 200, 600, 1000, 1500, 2000
3	7	29	50, 200, 600, 1000, 1500, 2000
4	4, 5, 6, 7, 8	27	1000

3.3.1 Effect of nozzle pressure ratio (NPR)

The effect of under-expanded and over-expanded nozzle flow on the near field pressure signature were computed for the hypersonic long-range transport vehicle. Changes in nozzle pressure ratio (NPR) will cause changes in the magnitude of the observed pressure signature, and then correspond to changes in the observed sonic boom signature.

In the condition of designed Mach number and flight altitude, a series of CFD simulation are obtained by varying nozzle pressure ratio (NPR) from 50 to 2000. All calculated conditions are illustrated in table 1 corresponding to the case2. The contour plots of symmetry plane static pressure for these states are given in Fig. 8. The pressure distributions taken at $h/L=1.15$ from the model are shown in figure 9. It is obviously that the change of NPR has little influence on the front shock wave except for NPR=2000, but as the rise of NPR, the intensity of aft shock waves increase visibly.

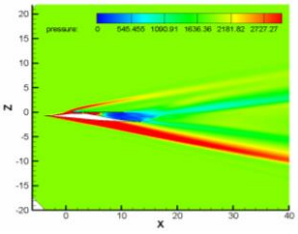

NPR=50

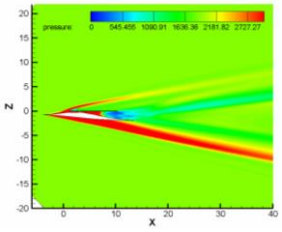

NPR=200

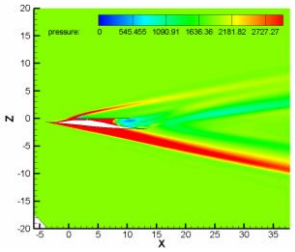

NPR=600

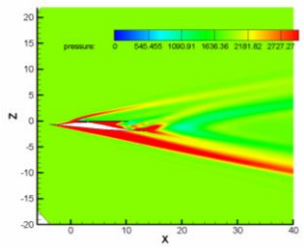

NPR=1000

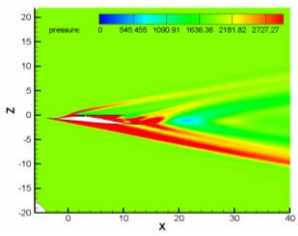

NPR=1500

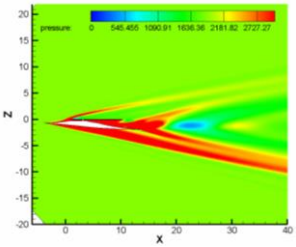

NPR=2000

Fig. 8 Symmetry plane pressure contours for different NPR, Ma=6, H=27km

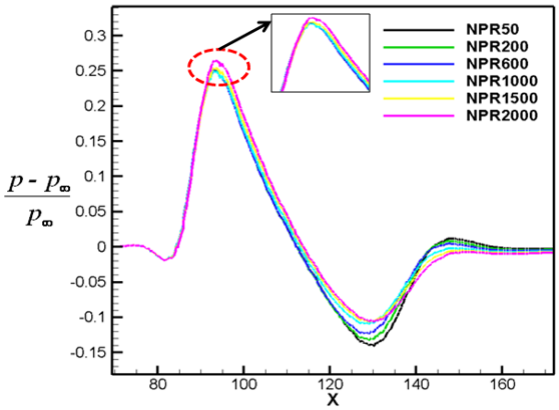

Fig. 9 Pressure distributions at $h/L=1.15$

Figure 10 shows what happens when far-field pressure signatures were propagated to the ground and the specific values considered are given in table 2. It is evident that as NPR increases, the dp(+) has slight increase except for NPR=2000, however the dp(-), peak-to-peak and time for the sonic boom on the ground decrease firstly and then increase. On the one hand, NPR has a major influence on the aft shock wave. But when the NPR is big enough, the engine exhaust nozzle plume effect on the front shock wave becomes obvious. On the other hand, in this flight Mach number and flight altitude, when the nozzle is under-expanded, reducing NPR helps reducing the intensity and duration of the sonic boom on the ground; when the nozzle is over-expanded, the increase of NPR is beneficial to reduce the

intensity and duration of the sonic boom on the ground.

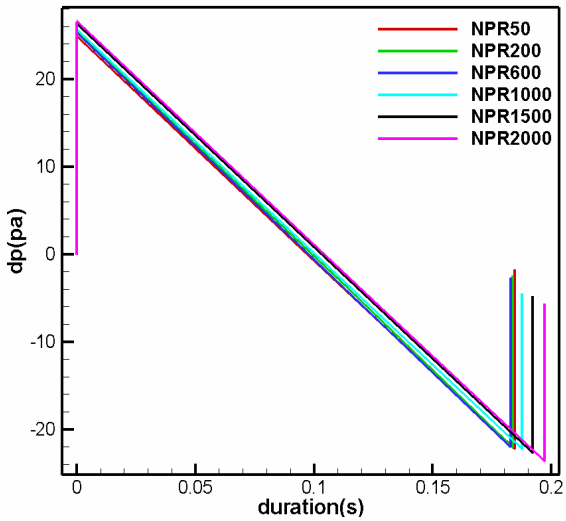

Fig. 10 The characteristic of sonic boom on ground for different NPR, Ma=6, H=27km

Table 2 Overpressure and duration on ground, Ma=6, H=27km

NPR	dp(+)/pa	dp(-)/pa	dp(+)-dp(-)/pa	duration/ms
50	24.910	22.250	47.159	184.516
200	24.951	22.085	47.036	183.716
600	25.600	21.982	47.582	182.781
1000	25.659	22.188	47.847	187.497
1500	25.670	22.689	48.358	192.221
2000	26.636	23.647	50.282	197.171

The above analysis is based on the designed Mach number and flight height. And then the parameters are changed according to the condition of equal dynamic pressure track.

The variation range of NPR is still 50~ 2000 and all calculated conditions are case1 and case3 in table 1. The contour plots of symmetry plane static pressure for case1 and case3 are given in figure 11 and 14 respectively. The pressures taken at $h/L=1.15$ from the model for case1 and case3 are shown in figure 12 and 15 respectively. Compared with case2, it can be seen that the near-field pressure characteristic has consistent trend with the increase of NPR in all Mach Numbers, which still has a great influence on the aft shock wave. But for the front shock wave, the higher the Mach number, the more significant the impact of NPR on it.

The characteristics of the sonic boom on ground are given in figure 13 and 16 respectively, and table 3 and 4 are the corresponding specific values considered. Compared with table 2, it can be found that the variable trends of all cases are consistent. As NPR increases within the present range, dp(+) increases gradually, and dp(-), peak-to-peak and time firstly decreases and then increases. However, the critical NPR of each Mach number is different. The critical NPR is 1000 for low Mach number, and 200 for high Mach number. That is, as the Mach number increases, the NPR value of the critical NPR decreases gradually.

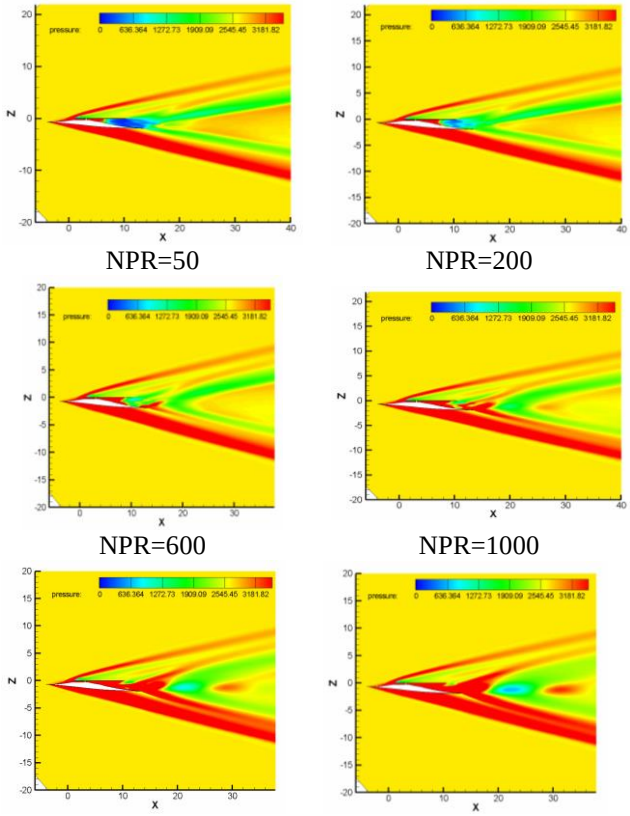

Fig. 11 Symmetry plane pressure contours for different NPR, Ma=5, H=24km

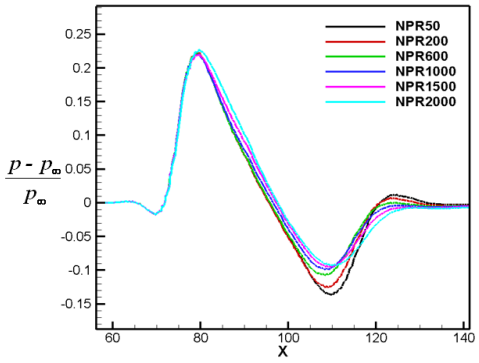

Fig. 12 Pressure distributions taken at $h/L=1.15$

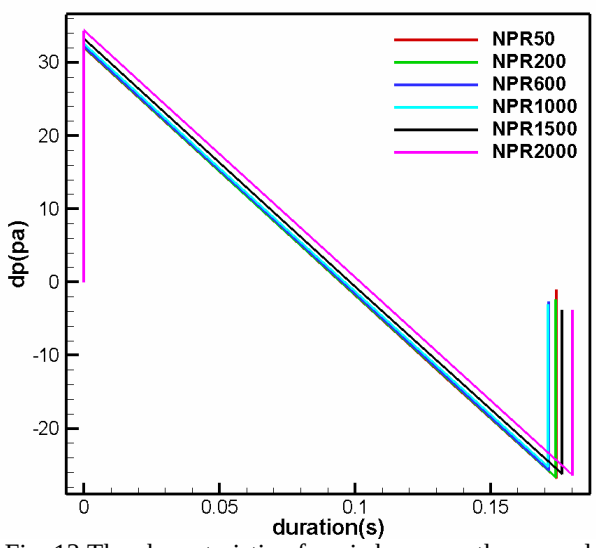

Fig. 13 The characteristic of sonic boom on the ground for different NPR, Ma=5, H=24km

Table 3 Overpressure and duration on ground Ma=5, H=24km

NPR	dp(+)/pa	dp(-)/pa	dp(+)-dp(-)/pa	duration/ms
50	32.042	26.791	58.833	174.277
200	32.115	26.635	58.750	173.969
600	32.158	25.667	57.823	171.482
1000	32.539	25.222	57.761	171.317
1500	33.239	26.221	59.460	176.321
2000	34.44195	26.3464	60.78875	180.235

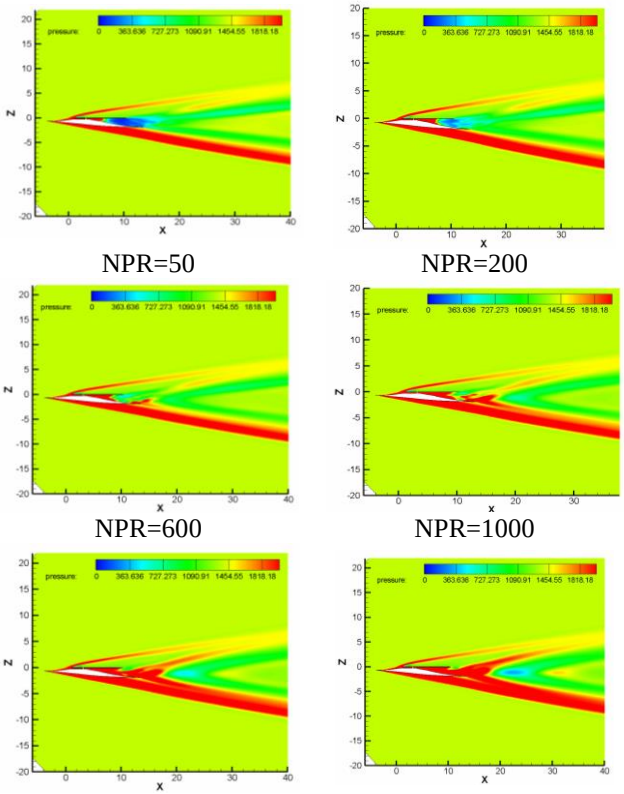

NPR=50 NPR=200

NPR=600 NPR=1000

NPR=1500 NPR=2000

Fig. 14 Symmetry plane pressure contours for different NPR, Ma=7, H=29km

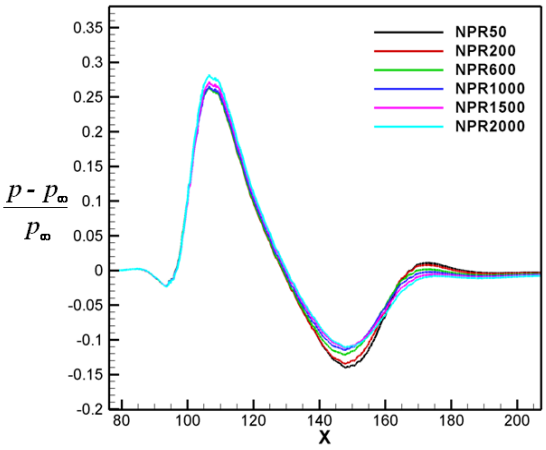

Fig. 15 Pressure distributions taken at $h/L=1.15$

Table 4 Overpressure and duration on ground Ma=7, H=29km

NPR	dp(+)/pa	dp(-)/pa	dp(+)-dp(-)/pa	duration/ms
50	22.303	19.135	41.439	193.723
200	22.232	18.909	41.141	192.277
600	22.308	19.111	41.418	193.503
1000	22.327	19.119	41.447	193.949
1500	22.578	19.700	42.279	197.912
2000	23.195	20.163	43.358	198.435

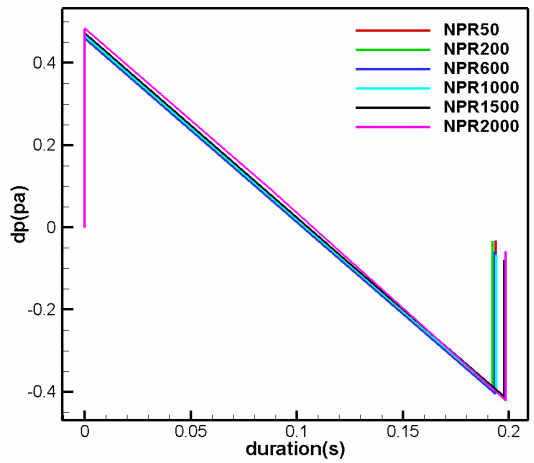

Fig. 16 The characteristic of sonic boom on ground for different NPR, Ma=7, H=29km

3.3.2 Effect of Mach number

To investigate the effect of Mach number on sonic boom overpressure, a series of CFD simulation are obtained by varying flight Mach

number from 4 to 8. All calculated conditions are the case4 which illustrated in table 1.

The contour plots of symmetry plane static pressure are given in Fig. 17. The pressure distributions extracted to set up the initial conditions for the far-field propagation algorithm taken at $h/L=1.15$ from the model are shown in figure 18, which shows that the near-field pressures increase gradually according to the increasing flight Mach number. The rise in front shock wave are 40.36% with Mach number range from 4 to 8, and the aft shock wave has 46.09% rise. So the aft shock is more sensitive to Mach number in the present cases.

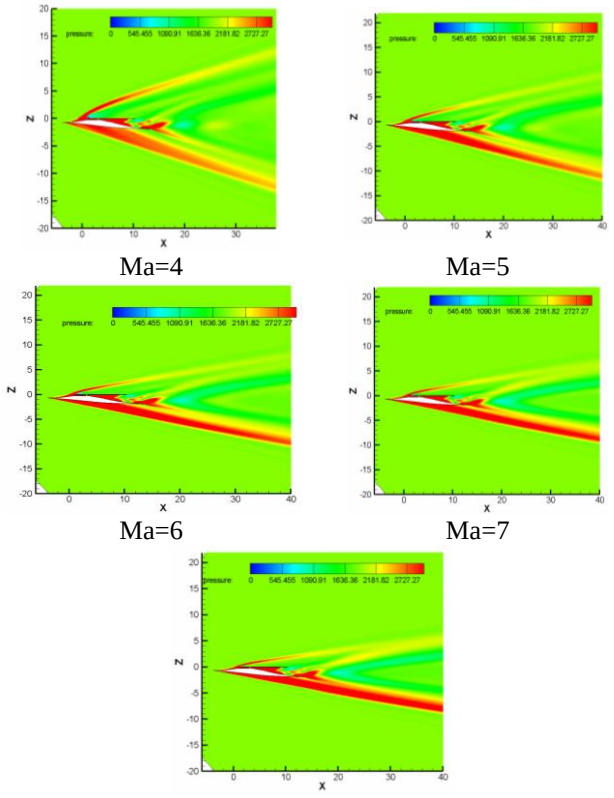

Fig. 17 Symmetry plane pressure contours for different Ma

The characteristic of the sonic booms on the ground are given in Fig. 19, and the specific parameters considered are given in table 5. It shows that the trend nearly linearly increase for all characteristics considered with increasing the Mach number. Furthermore, the growth rate for the aft shock wave is greater than the front shock wave. This is in accord with the change rule of the near-field pressure.

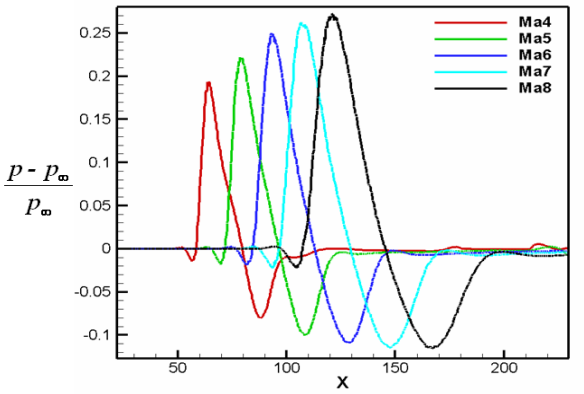

Fig. 18 Pressure distributions taken at $h/L=1.15$

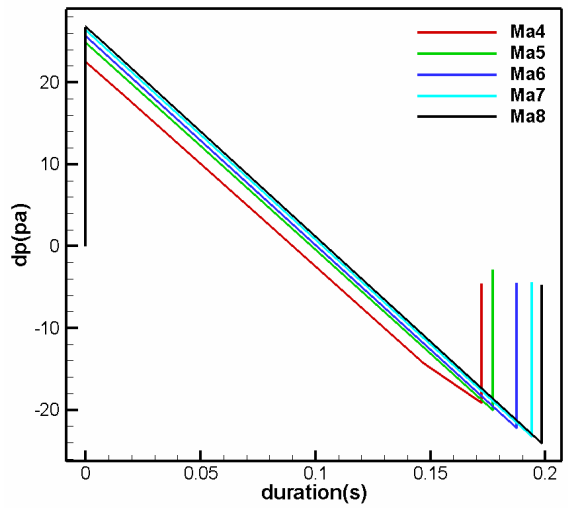

Fig. 19 The characteristic of sonic boom on ground for different Ma, NPR=1000, H=27km

Table 5 Overpressure and duration on ground NPR=1000, H=27km

Ma	dp(+)/pa	dp(-)/pa	dp(+)-dp(-)/pa	time/ms
4	22.533	19.179	41.712	172.23
5	24.897	20.029	44.927	177.082
6	25.659	22.188	47.847	187.497
7	26.421	23.274	49.696	194.106
8	26.845	24.104	50.9493	198.632

4 Conclusions

For the ground sonic boom prediction, near-field at the flight altitude are modeled by the conservative Navier-Stokes equations, and the far-field region computations are carried out using the Thomas ray tracing method. Based on the hypersonic long-range transport vehicle, nozzle pressure ratio (NPR) and Mach number are considered for investigating their effects on

the sonic boom signature including overpressure and time duration. According to the parametric analysis, it is found that:

i. In the design states， it is evident that as NPR increases, the dp(+) has slight increase except for NPR=2000, however the dp(-), peak-to-peak magnitude and time for the sonic boom on the ground decrease firstly and then increase.

ii. In the non-design states，the change trend of the two cases is consistent with design states. As NPR increases, dp(+) increases gradually, and dp(-), peak-to-peak and time firstly decreases and then increases. However, the critical NPR of each Mach number is different. The t critical NPR is about 1000 for low Mach number, and 200 for high Mach number. That is, as the Mach number increases, the critical NPR decreases gradually.

iii. In the case of same flight altitude and NPR, the characteristic considered of the sonic boom on the ground linearly increases gradually with increasing the flight Mach number. Furthermore, the growth rate for the aft shock wave is greater than that for the front shock wave. This is in accord with the change rule of the near-field pressure.

Acknowledgements

This work is supported by the National Natural Science Foundation of China (Grant No. 11672280)

Copyright Statement

References

[1] Maglieri D J, Plotkin K J. Sonic boom, chapter 10, aeroacoustics of flight vehicles [R]. *NASA RP-1258*, 1991, 1: 519-561.

[2] Hearing, E. A. Jr., Murray, J. E., Purifoy, D. D., Graham, D. H., Meredith, K. B., Ashburn, C. E., and Lt. Col. Stucky, M. Airborne shaped sonic boom demonstration pressure measurements with computational fluid dynamics comparisons, AIAA-2005-0009, 2005.

[3] Xu Zhifu, Li Xuefei, Xiang Xianhong, Qian Zhansen. Numerical simulation study on boundary layer spillage slot flow control for GK01 hypersonic inlet. Proceeding of the 15th Chinese Computational Fluid Dynamics Conference, PP: 1041-1046, Yantai, China, July 2012 (in Chinese).

[4] Li Hongmiao, Qian Zhansen, et al. Implementation of three different transition methods and comparative analysis of the results computed by OVERSET software. AIAA Paper 2016-3491, 2016.

[5] http://www.pointwise.com

[6] Thomas C., Extrapolation of sonic boom pressure signatures by the waveform parameter method, TND-6832, 1972.

[7] Thomas, Charles L. Extrapolation of wind-tunnel sonic boom signatures without use of a Whitham F-Function. NASA SP-255, 1970, pp. 205-217.

[8] Qian Zhansen, Yang Ximing. Key aerodynamic technologies of high Mach number civil transport. Proceeding of Young Research Conference of the 5th International Forum of Aviation Research, Zhuhai, China, November 8th-11th, 2014

[9] Xiang Xianhong, Gao Liangjie, Qian Zhansen. A type of truncated busemann inlet for a long-range hypersonic cruise aircraft. 13th China-Russia aviation technology academic conference, Moscow, 2013, 09.

[10] Carlson H. W., Mack R. J. and Morris O. A., A Wind-Tunnel Investigation of the Effect of Body Shape On Sonic-Boom Pressure Distributions, NASA TN D-3160,November 1965.

[11] Leng Yan, Qian Zhansen. A CFD based sonic boom prediction method and investigation on the parameters affecting the sonic boom signature. Proceeding of 2014 Asia-Pacific International Symposium on Aerospace Technology, Shanghai, China, August 22nd-24th, 2014.

[12] Raymond C. Exhaust Nozzle Plume Effects on Sonic Boom. Journal of aircraft, Vol. 49, No. 2, March–April 2012.

[13] Raymond C. Nozzle Plume Effects on Sonic Boom Test Results for Vectored Nozzles. AIAA Paper 2011-5974, 2011.

[14] Leng Yan, Qian Zhansen. Sonic boom signature prediction and analysis for a type of hypersonic long-range civil vehicle. AIAA Paper 2017-4422, 2017